Incorporation of Fe(iii) into Bentonite and study of its As^{3+} adsorption properties

B. K. Yadav* and V. K. Jha*

*Central Department of Chemistry, Tribhuvan University, Kirtipur, Kathmandu, Nepal.

Abstract: Bentonite is montmorillonite type layered clay and has high cation exchange capacity (CEC) because of its typical layered silicate structure. The bentonite was treated with hydrochloric acid to obtain H-bentonite which was further modified by incorporating Fe(III) into it. The modified Fe-bentonite was characterized by XRD and FTIR analyses. The specific surface area of the Fe-bentonite adsorbent was obtained from Methylene Blue Adsorption Method and was 598 m^2/g.

The adsorption of As^{3+} by Fe-bentonite adsorbent in aqueous environment was investigated by varying different experimental parameters such as pH, contact time and adsorption isotherm. The adsorption process was found to be best fitted to Langmuir adsorption isotherm model controlled by pseudo-second –order kinetics with the rate constant value 0.03723 g/(mg.min). The maximum arsenic adsorption was observed at pH 5 at room temperature. The time taken to reach equilibrium was 75 minutes. The maximum adsorption capacity for As^{3+} on Fe-bentonite was 101.01 mg/g. The value of ΔG (-21 kJ/mole) confirmed the adsorption process was favored by physiosorption. The slope of the linear plot of Q_t vs $t^{0.5}$ was linear but not passed through the origin, which indicated that, the intraparticle diffusion was not only rate controlling step.

Keywords: Modified bentonite; Montmorillonite; Pillaring; Rate constant.

Introduction

One of the most valuable substances on Earth is the clean water suitable for human consumption. The careless treatment and the poisoning of drinking water sources cause an enormous problem around the world[1]. Most of our water bodies have become polluted due to industrial growth; urbanization and manmade problems mainly the result of population growth. Poor sanitation and contaminated drinking water arising from human activity and natural phenomena create serious problems in human health[2]. The water sources are getting polluted day by day due to sewage and other waste, industrial effluents, agricultural discharges and industrial wastes from chemical industries, fossils fuel plants and nuclear power plants[2]. These contaminants create a large problem of water pollution rendering water no longer fit for drinking, agriculture as well as for aquatic life[3].

Most rivers in Nepal's urban areas have been polluted and their water are now not fit for human use, whereas drinking water in Kathmandu is contaminated with coliform bacteria, iron, ammonia and other contaminates according to UN reports presented at the 3rd world war forum in Japan[4].

The surface water in the Kathmandu valley is severely polluted by industrial effluence, domestic waste, and by the discharge of untreated sewage from residential areas. The effluent discharged by the factories contains detergents, non-biodegradable material and toxic chemicals hazardous to health and hygiene[3]. In some of the rural regions of Nepal communities still rely on getting their drinking water from tube wells. Recently one of the major concerns in the regions of Terai is ground water contamination from arsenic[5]. Even though out of total population of Nepal an estimated 84% people have access to safe drinking water, it is not safe. In rural areas of Nepal, millions of people do not have access to safe drinking water or basic sanitation sources. Only 27% of the population as a whole has access to sanitary facilities[3].

Author for correspondence: Vinay Kumar Jha, Central Department of Chemistry, Tribhuvan University, Kritipur, Kathmanu, Nepal.
Email: vinayj2@yahoo.com

Received: 30 April 2023; Received in revised form: 02 July 2023; Accepted: 05 July 2023.
Doi:https://doi.org/10.3126/sw.v16i16.56767

The heavy metals are toxic and detrimental water pollutants. The industrial wastewater contains the variety of inorganic compounds which are characterized as toxic, carcinogenic and mutagenic which when persist in the environment have the potential to cause adverse effect on human beings and animals and vegetation because of their mobility in aqueous ecosystem, toxicity and non-biodegradability. The heavy metals present in the industrial waste water such as Pb, Cd, Cr, Ni, Zn, and As are the most toxic among the other toxic materials from the chemical and allied industries[6].

Arsenic belongs to group VA in the Periodic Table with symbol As having atomic number 33 and atomic weight 74.92[7]. Arsenic, a metalloid, possesses both metallic and non metallic properties, is ubiquitously present in air, soil, natural water, mineral deposits and rocks and biota in varying concentrations. It can be released into the environment by both natural and anthropogenic processes. Natural processes are volcanic emissions, biological activities, burning of fossil fuels and weathering of arsenic bearing rocks and minerals such as realgar (AsS), orpiment (As_2S_3), arsenopyrite (FeAsS), and lollingite ($FeAs_2$). Anthropogenic sources include applications of arsenical pesticides, insecticides wood preservatives, paints, drugs, dyes, semiconductors, incineration of arsenic containing substances, industrial wastewater discharge, mine tailing/landfill leaching, and manufacturing of arsenic compounds[8].

Arsenic can be present both in inorganic and organic forms depending on the ambient environment and microbial activity[8]. Arsenic is usually found in combined form as inorganic and organic arsenic. Arsenic, combined with elements such as oxygen, chlorine and sulphur, is termed to as inorganic arsenic. Arsenic combined with carbon and hydrogen termed to as organic arsenic. Organic species of arsenic include in the form of mono-methyl arsenic acid (MMAA) and dimethyl arsenic acid (DMAA). Inorganic arsenic exists in As(III) and As(V) states. In ground water As usually exist as arsenite [As(III)] and arsenate [As(V)], where As(III) is predominant species which is more toxic and more difficult to remove than As(V)[9].

Arsenic occurs in several oxidation states as 0, +5, +3, and -3 in aqueous media[9]. Naturally occurring inorganic arsenic is stable in oxidation state of -3 as in arsine gas (AsH_3), 0 as in crystalline/elemental arsenic,
+3 as in arsenite, and +5 as in arsenate. The elemental state is extremely rare whereas -3 oxidation state is found only in extremely reducing conditions. Arsenate species are stable in oxygenated waters. Under mildly reducing conditions, arsenite predominates[8].

Arsenic is one of the most toxic and carcinogenic elements polluting water sources[10]. The regulatory authorities like the World Health Organization (WHO) and United States Environmental Protection Agency (USEPA) have reduced the maximum permissible concentrations level (MCL) of total arsenic in drinking water from 50 to 10 µg/L. However, much higher concentrations of arsenic than the permissible limit still exist in many parts of the world such as Argentina, Bangladesh, India, Pakistan, Mexico, Mongolia, Germany, Thailand, China, Chile, USA, Canada, Hungary, Romania, Vietnam, Nepal, Myanmar, and Combodia[8].

In 1999, Department of Water Supply and Sanitation (DWSS), in assistance with WHO, conducted first study on arsenic contamination in the eastern Terai region of Nepal. The study showed the availability of arsenic contamination in groundwater of Terai. Low level of Arsenic concentration was reported in Ilam, Morang, Udaypur, Mahottari, Kathmandu, Parsa, Lalitpur, Chitwan, Palpa, Dang, and Bardia whereas more than 50 ppb arsenic concentration is reported mostly in drinking water samples collected from Nawalparasi, Rautahat, Bara and Kailali districts of Nepal[11].

Exposure to high level of arsenic causes acute and chronic poisoning. Human exposure of As takes place through inhalation or skin absorption, ingestion. Inorganic As is readily absorbed from the gastro intestinal tract and becomes distributed throughout the body, tissues and fluids[12]. Excess availability and long term exposure to arsenic may lead to the development of various diseases such as conjunctivitis, hyperkeratosis, hyperpigmentation, cardiovascular diseases, disorders of the central nervous system and peripheral vascular system, skin lesions, lungs,

kidney cancer, and gangrene of the limbs. Epidemiological studies also reported that excess exposure to the aforementioned chemical species may interfere with metabolic activities of living organisms; consumption of those chemicals may also accelerate multisystem organ failure by allosteric inhibition of sulfhydryl enzymes that are essential for regulating metabolic activities, hence leading to death[13].

Several chemical and physical techniques have been used and developed to remove high concentration of toxic heavy metals from wastewater including: precipitations, solvent extraction, ion-exchange, reverse osmosis, oxidation/reduction, sedimentation, filtration, electrochemical techniques, cation surfactant, etc. However, these methods have certain performance limitations like high operational cost, low removal efficiency at low concentration and toxic sludge generation which requires additional treatment[14].

Current research has focused on the adsorption process. It is a simple, cost effective, more readily available, having high efficiency, easy handling and environment friendly. Adsorption is the alternative process for heavy metal removal due to the wide number of natural materials or agricultural wastes gathering in abundance from our environment[15].

Thus, the researchers are interested to search for low cost and locally available materials as adsorbent for metal ion removal from the wastewater. However, efforts have been contributed to develop new adsorbent and improve the existing adsorbent to have an alternative to activated carbon[16]. The development of novel adsorbents generally involves in new technology for arsenic removal from the contaminated water or waste water[17]. Various materials such as zeolites, clays, activated carbon, biomaterials, metal oxides, zero- valent iron and neutralized red mud have been used as adsorbents to remove arsenic from contaminated water and waste water[18].

Among them, clays, due to their inexpensive, acceptability, applicability, abundance and high adsorption efficiency, have been received much attention in removal of heavy metals from contaminated water[18]. Bentonite modified either with Fe, Al, or Mn salts showed significant improvements in adsorption affinity for arsenic by which the removal percentage of As^{3+} ranged from 92 to >99% with the corresponding adsorption capacity up to 4.5 mg/g[19]. Clay pillared with Titanium(IV), Iron(III) and Aluminum(III) showed similar adsorption capacities for As(V) but differences in adsorption capacities for As(III)[20]. Recently, arsenic adsorption on the raw clay modified with cationic surfactants has been received much more attention. The organo-clays are prepared by exchange of Na^+ or Ca^{2+} cations with cationic surfactants participated on the surface of clays, where charge on the clay surface is reversed from negative to positive. The positively charged head groups are balanced by counter anions (A^-), which makes the raw clay modified with cationic surfactants to be a potential adsorbent to adsorb anionic contaminants, such as arsenate oxyanions via ion exchange mechanism[18, 21].

There are wide varieties of raw clay minerals present in nature. Most of them are used in laboratory as adsorbent such as modified bentonite with different cations, Na^+-bentonite, Ca^{2+}-bentonite, Mg^{2+}-bentonite, zeolites, polymer muds etc. These all adsorbents were used to remove heavy metal ions from the contaminated water.

Various studies shows that Fe-bentonite also adsorbed large number of heavy metals. Hence this incident encouraged studying the adsorption property of the Fe-bentonite clay materials. Recently, the studies of the adsorption on the raw clay modified with cationic surfactant has been received much more attention, because of the different raw clay minerals are abundant in nature and are inexpensive. These materials are used in the adsorption technology to remove different non-biodegradable and toxic elements from the contaminated water or from environment.

Materials and Methods

Preparation of Fe-Bentonite

Bentonite clay (*100% pure Bentonite Wyoming, USA*) was dried at temperature 110 °C for one hour and then 50 g of bentonite was mixed with 150 mL of H_2O_2 with continuous stirring to make slurry and to remove organic matter. The slurry was washed thoroughly with distilled water 4 to 5

times and then dried in to dry oven at temperature 110 ℃ for one hour. The dried sample was ground using mortar and pestle until a fine powder like structure was obtained. In the powdered sample 100 mL of 0.1M hydrochloric acid was mixed to make slurry. Here HCl was added to exchange the various cations with H^+ ions present in the slurry. Again, it was washed thoroughly with distilled water until all the acidic chloride ions were removed from the solution and solution becomes neutral. The washed sample was again dried at 110 ℃ for 24 hours and then ground using mortar and pestle. In fine powder of sample, 0.1M of $FeCl_3$ was treated and allowed to stand for one hour and the solution was again washed with distilled water until the solution becomes neutral. Then, it was dried in air dry oven at 110 ℃ for overnight and the dried sample was ground to make a fine powder using mortar and pestle.

The schematic diagram of the preparation of Fe-bentonite is shown in Figure 1.

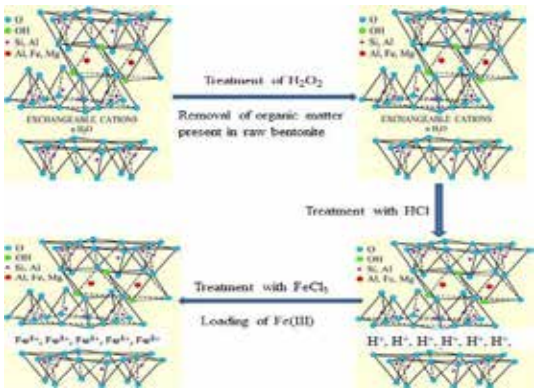

Figure 1: Schematic diagram of preparation of Fe-bentonite.

Preparation of stock and standard solutions

Stock solution of As(III) 1000 ppm from arsenic trioxide (As_2O_3, LR Grade Loba Chemie, dried at 110 ºC for an hour) was prepared. The standard arsenic solutions of required concentration were prepared by appropriate dilution of stock arsenic solution by adding 1 mL HCl in volumetric flask.

Ammonium molyddate reagent (I) 500 mL was prepared from ammonium heptamolybdate [$(NH_4)_6M_{O7}O_{24}.4H_2O$, LR Grade Qualigens 87.5 mL], 140 mL of Conc. sulphuric acid in distilled water cautiously[7, 22].

Ammonium molybdate reagent (II) was prepared from ammonium molybdate (20.05 g). Ammonium molybdate reagent (I) (198 mL) was added to the reagent (II), cooled and diluted up to 500 mL with distilled water. The concentration of the reagent (II) was 5%. The 0.5 M ammonium molybdate working solution was prepared from dilution method[7, 22].

The potassium permanganate ($KMnO_4$, LR Grade, Qualigens) solution of 0.1 N was prepared

The 1.5 N sulphuric acid 250 mL was prepared in distilled water.

The 0.5 M hydrazine hydrate solution was prepared by taking 2.44 mL and diluted to 100 mL.

Buffer solutions of pH 4.0, 7.0 and 9.2, were employed for calibration of pH meter.

Adsorption Studies

Preparation of Calibration Curve for Methylene Blue Solution

For preparation of calibration curve, at first the maximum absorbance was designed. Here it was done by preparing 5 mg/L solution of methylene blue. The absorbance was measured against wavelength ranging from 600 to 690 nm using spectrophotometer (Aquarius, CE 7200, England). The maximum absorbance (λ_{max}) obtained was at 665 nm. After that the methylene blue solution of 1 to 12 mg/L were prepared in 25 mL volumetric flasks. The absorbance of all these solutions was taken at 665 nm wavelength. A plot of absorbance versus concentration thus gives a calibration curve for methylene blue solution.

Specific surface area determination

To determine the specific surface area of the raw and activated carbons, the Langmuir adsorption isotherm model was used. For this, 0.05 g of Fe-bentonite was weighed out accurately and transferred to reagent bottles containing varying concentration of methylene blue (MB) solutions (50-400 mg/L).

The absorbance of the resultant solutions was taken at 665 nm wavelength. From the Langmuir adsorption isotherm,

Q_m value was calculated and using the formula of specific surface area equation (1)[23], the specific surface area of Fe-bentonite was determined.

$$S_{MB} = \frac{N_g \times a_{MB} \times N \times 10^{-20}}{M} \quad \ldots\ldots\ldots \quad (1)$$

Where, S_{MB} is the specific surface area in 10^{-3} km^2 kg^{-1}. The Q_m is the amount of adsorbate per unit gram of adsorbent required to form a monolayer coverage, a_{MB} is occupied surface area of one molecule of MB = $197.2A^2$, N is Avogadro's number (6.023×10^{23}), M is the molecular weight of MB (319.85 g/mol).

Preparation of calibration curve of As^{3+} ion

For the preparation of calibration curve of As^{3+}, Arsenic solution containing 0.1 to 0.9 mg/L and blank solution were prepared in 25 mL volumetric flask by following methods:

The required amounts of diluted solutions were pipetted out and transferred into 25 mL volumetric flasks to each solution 4.5 mL of 1.5 N sulphuric acid was added then one drop of 0.1 N potassium permanganate was added, stirred for one minute. Three mL of 0.5% ammonium molybdate and 3 mL of 0.5 M hydrazine hydrate were added. The volume was made up to mark by adding distilled water. In order for full color development, the above solutions were left for 20 minutes at room temperature. The absorbance of each solution was measured at 840 nm against blank solution with the help of spectrophotometer. A plot of absorbance versus concentration of arsenic was made.

Effect of pH

For the pH of As^{3+} adsorption, the initial concentration and volume of solution were taken 20 mg/L and 50 mL respectively. The solutions were taken in 100 mL Erlenmeyer flask and pH of the solution was adjusted from 2 to 8 separately using 0.1 M NaOH and HCl solutions by the help of pH meter. To each flask, 0.05 g of Fe(III) loaded bentonite adsorbent was added and then shaken in mechanical shaker for 24 hours at speed 220 rpm. After shaking, each solution was filtered immediately using Whatman No. 41 filter paper and the equilibrium pH of the filtrate was noted. The filtrate was analyzed to determine the equilibrium concentration of arsenic with the help of initial and equilibrium concentrations, the percentage adsorption of As^{3+} was evaluated.

Adsorption Isotherm Studies

For the study of isotherm studies of As^{3+} the effect of arsenic concentrations on the adsorption was studied under optimum pH. The adsorption isotherm study was done with different initial concentrations of As^{3+} ion ranging from 10 to 100 mg/L with 0.05 g of Fe-bentonite adsorbent. The solutions were shaken in a mechanical shaker for 24 hours at speed of 200 rpm. The equilibrium concentrations of arsenic after adsorption were determined by molybdenum blue method using spectrophotometer. Two models Langmuir model and Freundlich model have been tested to study the adsorption isotherm study.

Kinetic Studies

The adsorption kinetics experiments were performed at corresponding optimum pH for As^{3+} ion by equilibrating. For this study, 50 mL of 20 mg/L arsenic solutions in 100 mL Erlenmeyer flask containing 50 mg Fe-bentonite adsorbent were used. These flasks were shaken for different length of time 2 to 120 minutes, in a mechanical shaker at speed of 220 rpm. The kinetics were investigated by taking out flask at desired period of contact time and immediately filtrated through Whatman No. 41 filter paper to obtain filtrates and the concentrations in the filtrates were determined spectrophotometrically. The data obtained was tested with pseudo-first order and pseudo-second order kinetic models.

X-ray Diffraction Measurement

The raw and Fe-bentonite clay samples without any adsorption were analyzed for the phase detection using X-ray Diffractometer with monochromatic CuKα radiation (D2 Phaser Diffractometer, Bruker, Germany) at Nepal Academy of Science and Technology (NAST). The samples were scanned at 2θ from 10 to 80º. The XRD analysis was done to determine the chemical structure of bentonite clay and the adsorbent material obtained from it.

Fourier Transform Infrared Measurement

The raw and Fe-bentonite clay samples prepared in different environments together with the sample after the adsorption of As^{3+} were analyzed by using Fourier transform infrared spectroscopy (IRTracer 100, Shimadzu, Japan) at Central Department of Chemistry, Tribhuvan University for the functional groups available in raw, Fe-bentonite and As^{3+} adsorbed bentonite clays.

Results and Discussion

Characterization of Adsorbent Materials

X-ray diffraction (XRD) analysis

The XRD patterns of raw and Fe-bentonite clay samples were recorded and shown in Figure 2.

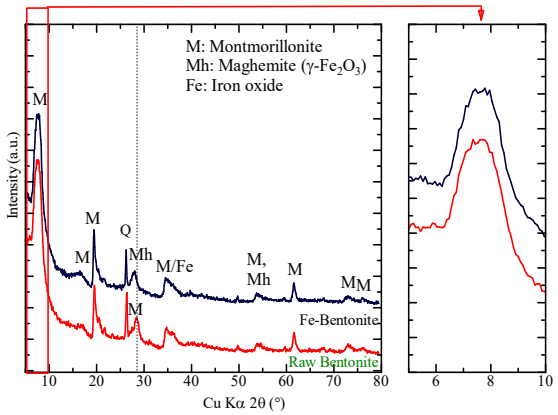

Figure 2: X-ray diffraction patterns of raw and Fe-bentonite clay.

The XRD patterns of raw and Fe-bentonite show the 2θ reflection peaks at 7.6, 16.5, 19.5, 28.3, 34.7, 53.8, 61.5, 73 and 76° which are the characteristics of Montmorillonite (bentonite is a type of montmorillonite clay) whereas the sharp peak at 2θ reflection angle of 26.3° is of quartz (SiO_2).

The shifts in the peaks from 28.3 to 27.97°, 34.7 to 34.5° and 53.8 to 53.7° are due to the loading of Fe(III) at the exchangeable sites in bentonite clay. Furthermore, the increase of the d-spacing of the major peak of montmorillonite/bentonite (7.6°) is expected to be due to the incorporation of Fe within the layered framework of bentonite clay.

Fourier Transform Infra-Red Spectra Analysis

The FTIR spectra of raw and Fe-bentonite clay samples are shown in Figure 3.

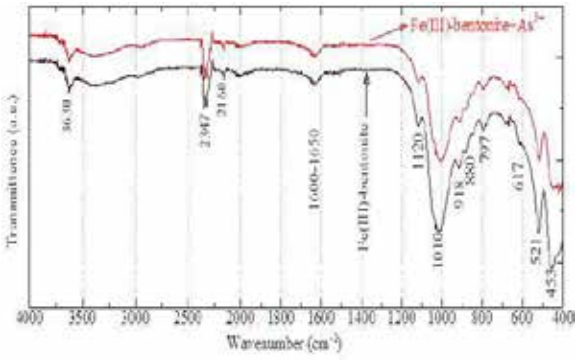

Figure 3: FTIR spectra of Fe-bentonite before and after As^{3+} adsorption.

The FTIR spectrum of Fe-bentonite prepared by loading of Fe(III) on raw bentonite showed main absorption at 3630, 2347, 2160, 1650-1600, 1317, 1120, 1010, 918, 880, 797, 617, 521 and 453 cm^{-1} and the mode of vibrations of the IR peaks appeared in FTIR spectra are of OH-stretching, CO_2 bond, H_2O bond, OH stretching and bending vibration of sorbed water molecules present in clay, Si-O-Si, Si-o stretching of silica and quartz, Al-O group, Al_2OH, Si-O-Mg stretching, Fe^{3+}-OH-Mg, and Si-O-Al (617, 521 and 453 cm^{-1}), respectively. No any appreciable change was observed in the FTIR spectra of adsorbent after As^{3+} adsorption.

The λ_{max} determination and calibration curve of Methylene Blue solution

The maximum absorbance was obtained at 665 nm from the plot of the absorbance of methylene blue with the variation of wavelength which is in trend with the previous report[24]. The calibration curve of methylene blue solution shows the linear relationship between the absorbance and the concentration up to 10 mg/L and thus follows the Beer Lambert's law. For higher concentrations of the methylene blue solution further dilution required.

Specific surface area determination

The linearized Langmuir plots for the adsorption of methylene blue on Fe-bentonite is shown in Figure 4 and the specific surface area calculated using Eqn. 1 was 598 m^2/g.

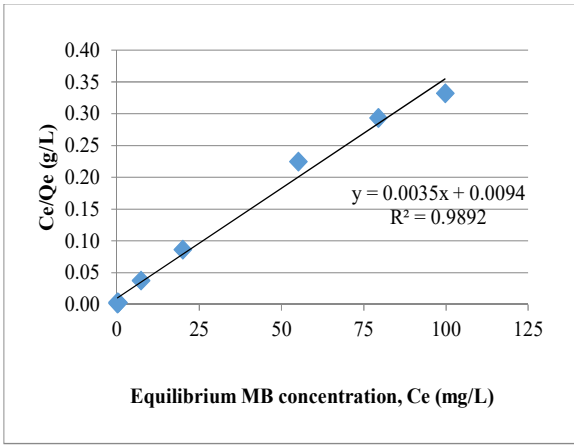

Figure 4: A plot of C_e/Q_e versus Ce of the Fe-bentonite clay.

Determination of λ_{max} and calibration of As^{3+} solution

The absorbance of As^{3+} solution with the variation of wavelength confirmed the maximum absorbance at 840 nm which is in trend with the previous report[24]. The calibration curve of As(III) solution showed that it obeys Beer-Lambert's law up to 6 ppm concentration of As^{3+}.

Effect of pH

The effect of pH for the adsorption of As^{3+} onto the Fe-bentonite adsorbent prepared in this study is shown in Figure 5.

The effect of initial pH on the adsorption of As^{3+} was studied in the rage from 2 to 8. The adsorption of As^{3+} was found increasing with increasing initial pH value from 2 up to 5 and then decreased with further increase the initial pH. The maximum adsorption of As^{3+} was found at initial pH 5 with the values 17.1 mg/g. The maximum adsorption of As^{3+} was expected to occur at pH 9 onto the Fe-bentonite clay adsorbent material but the maximum adsorption of As^{3+} was found at pH 5. This is the fact that when at the initial pH values <9.0, the predominant form of As^{3+} in the solution is H_3AsO_3, and anion exchange is not a major mechanism but it is a physical adsorption through Si-O and Al-O groups at the edges of the clay particles and may be due to partially ion-exchange process. For further experimental works, the adsorption of As^{3+} onto the present Fe-bentonite clay adsorbent material, the optimum pH value was set to pH 5.

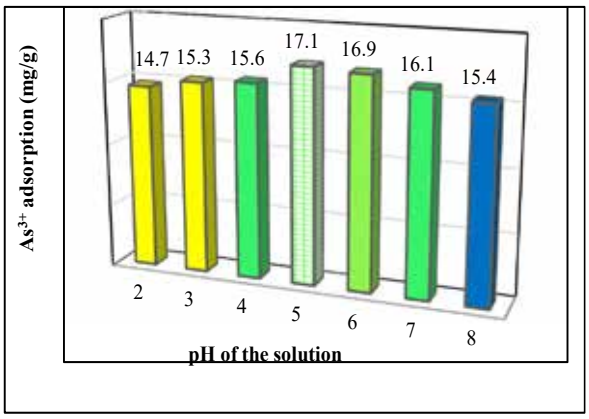

Figure 5: Adsorption of As^{3+} on Fe-bentonite as a function of initial pH of the solution.

Adsorption isotherm of As^{3+}

Adsorption isotherm is a pictorial representation of the amount of adsorbate adsorbed per unit mass of the adsorbent as a function of the amount of adsorbate left in bulk solution at equilibrium at constant temperature. Several models have been developed to describe the adsorption phenomenon but the Langmuir and Freundlich adsorption isotherms are the well-known models used to analyze adsorption behavior.

In 1918, Langmuir gave the first quantitative model of adsorption. This model has been successfully applied for the adsorption of solute from a liquid solution on homogeneous adsorbent with the formation of monolayer coverage and adsorption is independent of the occupation of neighboring sites[25]. The Langmuir isotherm is used to estimate the maximum adsorption capacity of complete monolayer coverage on the adsorbent surface. The linearized form of Langmuir adsorption isotherm is given by the following equation:

$$\frac{C_e}{Q_e} = \frac{1}{Q_m b} + \frac{C_e}{Q_m} \quad \cdots \quad (2)$$

Where Q_e (mg/g) is the amount of adsorbate adsorbed per unit mass of adsorbent at equilibrium, C_e (mg/L) is the equilibrium concentration of the adsorbate, Q_m (mg/g) is the maximum adsorption capacity and 'b' (L/mg) is the Langmuir adsorption equilibrium constant.

A plot of C_e/Q_e against C_e gives a straight line with slope $1/Q_m$ and intercepts $1/Q_m b$ from which Q_m and 'b' can be determined.

The essential characteristics of Langmuir isotherm can be expressed in terms of dimensionless constant separation factor or equilibrium parameter R_L defined by relation[26],

$$R_L = \frac{1}{(1 + bC_i)} \quad \cdots \quad (3)$$

Where, b = Langmuir constant and C_i = Initial concentration of As^{3+}.

The equilibrium parameter, R_L indicates the shape of isotherm and nature of the adsorption process (R_L>1 unfavorable, R_L = 1 linear, 0 <R_L< 1 favorable, R_L = 0 irreversible). The value of R_L between 0 and 1 indicates that adsorption is favorable. However, the Langmuir model gives no mechanistic aspects of adsorption.

The adsorption data obtained can also be analyzed with Freundlich adsorption isotherm model which was established in 1939[27]. The linear form of the Freundich isotherm is given by the equation:

$$log\ Q_e = log\ K_F + \frac{1}{n} log\ C_e \quad \cdots \quad (4)$$

Where Q_e (mg/g) is the amount of adsorbate adsorbed per unit mass of adsorbent, C_e (mg/L) is the equilibrium concentration of the adsorbate, K_F [(mg/g) (L/mg)$^{1/n}$] and n (g/L) are Freundlich equilibrium coefficients, which are considered to be the relative indicators of adsorption capacity and adsorption intensity. The logQ_e is plotted against log C_e a straight line is obtained with slope 1/n and intercept log K_F. From this plot, the value of 1/n and K_F can be determined. The value of 1/n between 0 and 1.0 indicates the favorable adsorption of adsorbate.

The adsorption study of As^{3+} onto Fe-bentonite was done at optimum pH 5 and varying the concentration of As^{3+} from 10-100 mg/L. The slopes and intercepts of the linearized Langmuir and Freundlich plots were used to calculate the Langmuir and Freundlich parameters for the adsorption of arsenic on the Fe-bentonite and shown in Table 1.

The coefficients of determination of Langmuir and Freundlich isotherms of As^{3+} were 0.9936 and 0.9860 respectively. Since the R^2 of Langmuir is greater than that of Freundlich, so the adsorption of As^{3+} ion is monolayer and involved the adsorption on homogeneous active surfaces. This implies that the experimental data fitted with the Langmuir model.

Table 1: Langmuir and Freundlich parameters and correlation coefficient with experimental Q_{max} for As^{3+}.

Langmuir isotherm				
Q_{max} (mg/g)	b (L/mg)	R^2	ΔG (KJ/Mol)	R_L
101.01	0.061	0.9936	-21	0.6146 to 0.1365
Freundlich isotherm				
K_F (L/g)		n		R^2
7.85		1.55		0.9860

The negative value of free energy (ΔG) in adsorption process reveals the spontaneous nature and feasibility of the adsorption process for the adsorption of As^{3+} onto Fe-bentonite clay. The values of ΔG confirms the adsorption process is favored by physio-chemical-adsorption for As^{3+}. The corresponding R_L values obtained from Table 1 for As^{3+} adsorption was found in between 0 and 1 which is in agreement with the favorable adsorption.

The adsorption of As^{3+} as a function of equilibrium concentration of As^{3+} is shown in Figure 6.

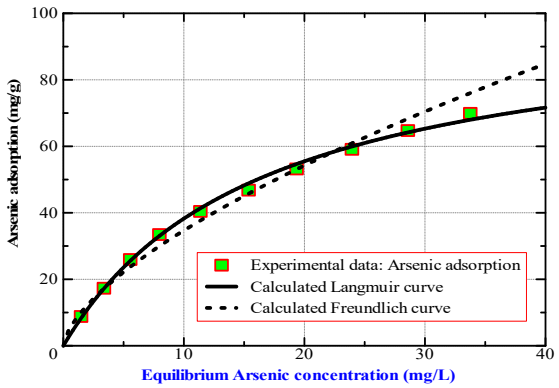

Figure 6: The adsorption isotherm of Arsenic onto Fe-bentonite.

The Q_m value obtained from Langmuir was found to be 101.01 mg/g, which is significantly higher than most of the

previously reported adsorbents but lower than Zr(V) loaded orange waste gel and steam activated banana peels shown in Table 2.

Table 2: Comparison of maximum adsorption capacity (Q_{max}) of the Fe-bentonite with earlier investigated adsorbents.

S. No.	Adsorbent and species	Q_{max} (mg/g)	Source
1	Phosphorylated orange juice residue	68.18	28
2	Spinacia oleracea (Spinach) Leaves	58.48	24
3	Fe loaded pomegranate waste	50.00	29
4	Zr(V) loaded orange waste gel	130.00	30
5	Thioglycolated sugarcane	0.085	31
6	Steam activated banana peels (i.e. N_2+H_2O-BP)	142.86	22
7	Fe-bentonite	101.01	This study

Kinetic studies

The study of adsorption kinetics describes the solute removal and the time required for the adsorbate removal at the solid-solution interface. The kinetic mechanism that controls the adsorption process onto Fe-bentonite was evaluated by using pseudo-first-order, pseudo-second-order and intraparticle diffusion models.

The differential form of pseudo-fist order rate equation which is applicable for the reversible reaction is generally expressed as[32]:

$$\frac{dQ_t}{dt} = K_1(Q_e - Q_t) \quad \cdots \quad (5)$$

Where, Q_e (mg/g) is the amount of adsorbate adsorbed at equilibrium and Q_t (mg/g) is the amount of adsorbate adsorbed at any time 't'. Similarly, K_1 (min^{-1}) is the rate constant of pseudo-first order adsorption.

After integration and applying boundary condition, t = 0 to t and Q_t = 0 to Q_t the linearized from of equation becomes:

$$\log(Q_e - Q_t) = \log Q_e - \frac{K_1}{2.303}t \quad \cdots \quad (6)$$

The plot of log (Q_e - Q_t) versus 't' should give a straight line from which K_1 and Q_e can be determined from slopes and intercepts of the plot respectively.

The pseudo-second order kinetic model is used to study the kinetics of adsorption of adsorbate, which states that the rate of occupation of adsorption sites is proportional to the square of the number if unoccupied sites[33]. It is generally expressed as:

$$\frac{dQ_t}{dt} = K_2(Q_e - Q_t)^2 \quad \cdots \quad (7)$$

Where K_2 (g/mg·min) is the pseudo-second order rate constant and Q_e and Q_t are the amount of adsorbate adsorbed at equilibrium and any time 't' respectively.

After integration and applying boundary conditions, t=0 to t and Q_t = 0 to Q_t the equation becomes:

$$\frac{1}{Q_t} = \frac{1}{K_2 Q_e^2} + \frac{1}{Q_e}t \quad \cdots\cdots\cdots \quad (8)$$

If the initial adsorption rate is V_0 (mg/g min), then

$$V_0 = K_2 Q_e^2 \quad \cdots \quad (9)$$

The equation can also be written as:

$$\frac{1}{Q_t} = \frac{1}{V_0} + \frac{1}{Q_e}t \quad \cdots \quad (10)$$

The values of Q_e and k_2 can be determined from the linear plot of t/Q_t versus 't' with the slope and intercept of the plot respectively.

The intraparticle diffusion model can be represented as[34]:

$$Q_t = K_i t^{1/2} \quad \cdots \quad (11)$$

Where, k_i is the intraparticle diffusion rate constant and Q_t is the amount of metal ion adsorbed (mg/ g) at time t (min). According to this model, the plot of q versus $t^{1/2}$ yields a straight line passing through the origin if the adsorption process obeys the sole intraparticle diffusion model.

With the help of the slopes and intercepts of the plots obtained from the equations (6) and (8), kinetic parameters of pseudo first and pseudo second order rate expressions of the adsorption of As^{3+} onto Fe-bentonite were calculated and are tabulated in the following Table 3:

Table 3: Kinetic Parameters of As^{3+} adsorption onto Fe-bentonite.

Pseudo First Order Model			Pseudo Second Order Model		
Q_e (mg/g)	K_1 (min^{-1})	R^2	Q_e (mg/g)	K_2 (g/mg min)	R^2
1.401	0.0272	0.9321	16.3	0.03723	0.9989

The coefficient of determination (R^2) values of pseudo-first order and pseudo-second order models of As^{3+} 0.9321 and 0.9989 respectively showed the kinetics of As^{3+} ion onto Fe-bentonite adsorbent followed pseudo-second order kinetics with the rate constant value 0.03723 g/mg min. The kinetics plot of the adsorption of As^{3+} onto Fe-bentonite is shown in Figure 7.

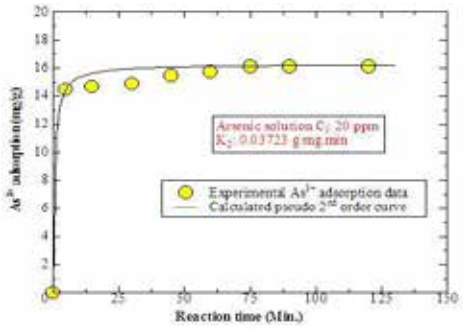

Figure 7: Kinetic plot for the adsorption of As^{3+} onto Fe- bentotinte.

It is very clear from the graphs that initially up to 10 minutes reaction time the process of adsorption was rapid and the equilibrium reached in 75 minutes minutes for As^{3+}. It was found that the adsorption rate of As^{3+} was rapid at first and then slowed down near the equilibrium state. After reaching the saturation point there was no significant change in the rate of adsorption.

The initial rapid increase in the rate was due to the availability of a greater number of active sites so that large number of As^{3+} ion got attached to adsorbent sites. As the time passed the number of active sites becomes less and finally the equilibrium state was reached.

The graphical relationship between the amount of As^{3+} adsorbed (mg/g) and square root of time (√t) (shown in Figure 8) does not pass through the origin which indicates that the intra-particle diffusion is not the rate limiting step.

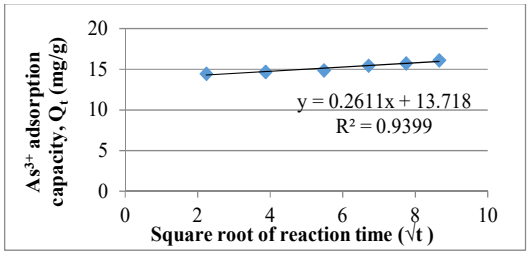

Figure 8: Plot of Q_t verses √t plot for the adsorption of As^{3+} on Fe-bentonite.

Conclusion

The Fe modified bentonite adsorbent material was prepared by Fe(III) loading/pillaring into the raw bentonite clay. Thus, prepared adsorbent material was characterized by FTIR, XRD analyses. The increase of the d-spacing of the major XRD peak of montmorillonite/bentonite (7.6°) is expected to be due to the incorporation of Fe within the layered framework of bentonite clay. The FTIR analysis concluded that the Si-O and Al-O groups at the edges of the clay particles and the Fe^{3+} ions present between tetrahedral layer of silicon and octahedral layer of aluminum bind the arsenic ion through the ion exchange process. The specific surface areas of Fe-bentonite estimated from methylene blue adsorption method was 598 m^2/g.

The maximum adsorption capacity of As^{3+} was found to be 101.01 mg/g at optimum pH 5. Langmuir and Freundlich isotherm models were tested to describe the adsorptions of As^{3+} onto Fe(III) loaded bentonite adsorbent. It was concluded that As^{3+} adsorption fitted well with the Langmuir isotherm (R^2 =0.9936).

The equilibrium contact time of As^{3+} was found to be 75 minutes following the pseudo-second order kinetic model with the rate constant value 0.03723 g/(mg·min) for As^{3+} ions adsorption. The value of ΔG obtained from Langmuir equation were -21 kJ/mol for As^{3+}. The negative value of free energy (ΔG) in adsorption process revealed that the spontaneous nature and feasibility of the adsorption process for the adsorption of As^{3+} onto Fe-bentonite. The value range of separation parameter R_L revealed good adsorption of As^{3+} onto Fe-bentonite.

Acknowledgements

We are grateful to Dr. Suresh Kumar Dhungel of Nepal Academy of Science and Technology (NAST) for the support to get X-ray diffraction measurement of our samples and Dr. Basant Giri of Kathmandu Institute of Applied Sciences for providing Wyoming bentonite clay.

References

[1] Buzetzky, D. et al. 2019. Application of modified bentonites for arsenite (III) removal from drinking water. *Periodica Polytechnica Chemical Engineering*. **63**(1): 113-121.

[2] Halder, J. N. and Islam, M. N. 2015. Water pollution and its impact on the human health. *Journal of Environment and Human.* **2**(1): 36-46.

[3] Pandey, S. 2006. Water pollution and health. *Kathmandu University Medical Journal*. **4**(1): 128-134.

[4] Jha, V. K., and Subedi, K. 2012. Preparation of activated charcoal adsorbent from waste tire. *Journal of Nepal Chemical Society*. **27**(1): 19-25.

[5] Wang, C. et al. 2019. Geographic inequalities in accessing improved water and sanitation facilities in nepal. *International Journal of Environmental Research and Public Health.* **16**(7): 1269-1281.

[6] Bobade, V. and Eshtiagi, N. 2015. Heavy metals removal from wastewater by adsorption process: A review. *Asia Pacific Confederation of Chemical Engineering Congress*.

[7] Karmacharya, M. S. et al. 2016. Removal of As(III) and As(V) using rubber tire derived activated carbon modified with alumina composite. *Journal of Molecular Liquids*. **216**: 836-844.

[8] Chowdhury, M. R. I. and Mulligan, C. N. 2011. Biosorption of arsenic from contaminated water by anaerobic biomass. *Journal of Hazardous Materials.* **190** (1-3): 486-492.

[9] Chang, Q., Linw. and Ying, W.C. 2010. Preparation of iron-impregnaled granular activated carbon for arsenic removal from drinking water. *Journal of Hazardous Materials.* **184**: 515-522

[10] Te, B., Wichitsathian, B. and Yossapol, C. 2017. Adsorptive behavior of low-cost modified natural clay adsorbents for arsenate removal from water. *International Journal of Geomate*. **12**(33): 1-7.

[11] Thakur, J. K., Thakur, R. K. 2010. Ramanathan, A., Kumar, M. and Singh, S. K., Arsenic contamination of groundwater in Nepal—an overview. *Water.* **3**(1): 1-2.

[12] Ratnaike, R. N. 2003. Acute and Chronic arsenic toxicity, *Postgraduate Medical Journal, Australia.* **79**: 391-396.

[13] Masindi, V. et al. 2014. Application of magnesite–bentonite clay composite as an alternative technology for removal of arsenic from industrial effluents. *Toxicological and Environmental Chemistry*. **96**(10):1435-1451.

[14] Matouq, M. et al. 2015. The adsorption kinetics and modeling for heavy metals removal from wastewater by Moringa pods. *Journal of Environmental Chemical Engineering*. **3**(2): 775-784.

[15] Petrović, M. et al. 2016. Removal of Pb^{2+} ions by raw corn silk (Zea mays L.) as a novel biosorbent. *Journal of the Taiwan Institute of Chemical Engineers*. **58**: 407-416.

[16] Park, J. et al. 2015. Competitive adsorption and selectivity sequence of heavy metals by chicken bone derived biochar, Batch and column experiment. *Journal of Environmental Science and Health.* **50**: 1194-1204.

[17] Mohan, D., and Pittman Jr, C. U. 2007. Arsenic removal from water/wastewater using adsorbents—a critical review. *Journal of Hazardous Materials*. **142**(1-2): 1-53.

[18] Su, J. et al. 2011. Synthesis, characterization and kinetic of a surfactant-modified bentonite used to remove As(III) and As(V) from aqueous solution. *Journal of Hazardous Materials*. **185**(1): 63-70.

[19] Ramesh, A. et al. 2007. Adsorption of inorganic and organic arsenic from aqueous solutions by polymeric Al/Fe modified montmorilonite. *Sorption and Purification Technology*. **56**(1): 90-100.

[20] Lenoble, V. et al. 2002. Arsenic adsorption onto pillared clays and iron oxides. *Journal of Colloid and Interface Science*. **255**(1): 52-58.

[21] Borah, D. et al. 2008. Surface-modified carbon black for As(V) removal. *Journal of Colloid and Interface Science*. **319**(1): 53-62.

[22] Maharjan, J. and Jha, V. K. 2022. Activated carbon obtained from banana peels for the removal of As (III) from water. *Scientific World*. **15**: 145-157.

[23] Itodo, A. U., H. U. Itodo and M. K. Gafar. 2010. Estimation of specific surface area using Langmuir isotherm method. *Journal of Applied Sciences and Environmental Management*. **14**(4): 141-145.

[24] Jha, P. K. and Jha, V. K. 2021. Arsenic adsorption characteristics of Adsorbent prepared from spinacia Oleracea (spinach) leaves. *Scientific World*. **14**: 51-61.

[25] Langmuir, I. J. 1918. The adsorption of gases on plane surfaces of glass, mica and platinum. *Journal of the American Chemical Society*. **40**: 1361-1403.

[26] Maron, S. H. and Pruton, C. F. 2001. *Principles of Physical Chemistry* (4th edition), Macmillan Company, New York.

[27] Freundlich, H. and Heller, W. 1939. The Adsorption of cis- and trans-Azobenzene. *Journal of American Chemical Society*. **61**: 2228-2230.

[28] Ghimire, K. N. et al. 2003. Adsorptive separation of arsenate and arsenite anions from aqueous medium by using orange waste. *Water Research*. **37**(20): 4945-4953.

[29] Thapa, S. and Pokhrel, M. R. 2012. Removal of As(III) from aqueous solution using Fe(III) loaded pomegranate waste. *Journal of Nepal Chemical Society*. **30**: 29-36.

[30] Biswas, B. K. et al. 2008. Adsorptive removal of As(V) and As(III) from water by a Zr(IV)-loaded orange waste gel. *Journal of Hazardous Materials*. **154**: 1066-1074.

[31] Roy, P. et al. 2013. Removal of arsenic(III) and arsenic(V) on chemically modified low-cost adsorbent: batch and column operations. *Applied Water Science*. **3**: 293-309.

[32] Lagergren, S. 1898. Zur theorie der sogenannten adsorption geloster stoffe. *Kungliga svenska vetenskapsakademiens. Handlingar*. **24**: 1-39.

[33] Ho, Y. S. and McKay, G. 1999. Pseudo-second order model for sorption processes. *Process Biochemistry*, **34**(5): 451-465.

[34] Karmacharya, M. S. 2017. *Physicochemical characteristics of activated carbon obtained from waste tire and its alumina composite*, PhD Thesis, Tribhuvan University, Kathmandu, Nepal.